Check for updates

Climate change or regional human impacts? Remote sensing tools, artificial neural networks, and wavelet approaches aim to solve the problem

Ehsan Foroumandi, Vahid Nourani and Elnaz Sharghi

ABSTRACT

Lake Urmia, as the largest lake in Iran, has suffered from water-level decline and this problem needs to be investigated accurately. The major reason for the decline is controversial. The current paper aimed to study the hydro-environmental variables over the Lake Urmia basin using remote sensing tools, artificial neural networks, wavelet transforms, and Mann–Kendall trend tests from 1995 to 2019 in order to determine the primary reason of the decline and to find the most important hydrologic periodicities over the basin. The results indicated that for the monthly-, seasonally-, and annually-based time series, the components with 4-month and 16-month, 24- and 48-month, and 2- and 4-year, respectively, are the most dominant periodicities over the basin. The agricultural increase according to the vegetation index and evapotranspiration and their close relationship with the water-level change indicated that human land-use is the main reason for the decline. The increasing agriculture, in the situations that the precipitation has not increased, caused the inflow runoff to the lake to decline and the remaining smaller discharge is not sufficient to stabilize the water level. Temperature time series, also, has experienced a significant positive trend which intensified the water-level change.

Key words | artificial neural networks, Lake Urmia, remote sensing, trend tests, water resources, wavelet transforms

Ehsan Foroumandi
Vahid Nourani (corresponding author)
Elnaz Sharghi
Center of Excellence in Hydroinformatics,
University of Tabriz,
Tabriz,
Iran
and
Faculty of Civil Engineering,
University of Tabriz,
Tabriz,
Iran
E-mail: *nourani@tabrizu.ac.ir*

Vahid Nourani
Faculty of Civil and Environmental Engineering,
Near East University, Near East Boulevard,
99138, N. Cyprus, via Mersin 10, Nicosia,
Turkey

HIGHLIGHTS

- The results indicate that for the monthly-, seasonally-, and annually based time-series, the components with 4-month and 16-month, 24- and 48-month, and 2- and 4-year, respectively are the most dominant frequencies over the Urmia lake basin.
- The results indicate that human land-use is the primary reason for the decline of the water-level. The increasing temperature, also, intensifies the water-level decline of the lake.

This is an Open Access article distributed under the terms of the Creative Commons Attribution Licence (CC BY 4.0), which permits copying, adaptation and redistribution, provided the original work is properly cited (http://creativecommons.org/licenses/by/4.0/).

doi: 10.2166/nh.2020.112

Downloaded from http://iwaponline.com/hr/article-pdf/52/1/176/846791/nh0520176.pdf
by guest

GRAPHICAL ABSTRACT

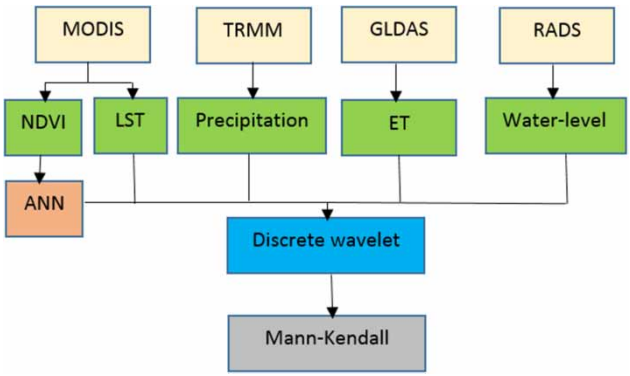

INTRODUCTION

The impacts of climate change and its effects have put stress on natural processes such as hydrological cycles, environmental variables, and ecological balance of the eco-systems (Erler *et al.* 2019), and global climate change is resulting in a thermodynamic intensification of the hydrologic cycles. While climate change is one of the reasons for hydro-environmental changes, human land- and water-use activities have affected water and land resources and have made a great many changes in the natural processes (Pokhrel *et al.* 2017). The over-use of water resources by humans causes socio-environmental problems, especially in semi-arid and arid regions such as the Middle East (Madani 2014). The main reasons for water resources problems are controversial among researchers due to the different approaches that they use to answer the question.

Iran, as a country in the Middle East, and due to the low annual precipitation, is situated among the semi-arid and arid regions. Located in the northwest part of Iran, Lake Urmia is the largest inland lake and has experienced rapid water-level decrement in the past years (Delju *et al.* 2013). The decline of the water-level equaled 8 m from 1995 to 2010, and up to 2012, the lake lost about 60% of its area and more than 90% of its volume, which makes the shrinking problem of Lake Urmia an outstanding tragedy in the Middle East (Hassanzadeh *et al.* 2012). The reason for the water-level decline is controversial and a great number of researchers have tried to answer the question. Several studies argue that the reduction of the surface water inflow due to excessive agricultural extraction caused the problem (e.g., see Alborzi *et al.* 2018; Nourani *et al.* 2018). Some other researchers proposed that building a large number of dams over the rivers which inflow to the lake has created the problem. This idea was triggered due to the extensive construction of reservoirs, although it was rejected in a paper written by Fathian *et al.* (2014), showing that decreasing trends were observed in the headwater catchment areas. Several other studies found that the climate change impacts over the region are the main cause of the decline in the water volume of Lake Urmia (e.g., see Delju *et al.* 2013; Tahroudi *et al.* 2019; Schulz *et al.* 2020).

Data gathering is one of the main processes in performing an accurate study. Various methods and indices are utilized to monitor and study hydrologic, environmental, and climate factors. These methods are divided into two main categories, which are remote sensing-based (RS-based) and site-based indices (Liu *et al.* 2016). Although some researchers use site-based tools to study trends in hydro-climatologic variables and climate change over regions, they are not available for every time and region due to the scarcity of ground-based data and they have low accuracy because of some disadvantages such as human mistakes and ungauged stations. One of the most important reasons for the disagreement among researchers about the reason for water resources problems is data. Using ground-based

Downloaded from http://iwaponline.com/hr/article-pdf/52/1/176/846791/nh0520176.pdf
by guest

data has several drawbacks. Moreover, using different ground-based stations, some of which are far away from each other, is confusing to study the same basin. Also, even in more recent studies, researchers used old datasets and they could not use near to real-time data to study trends in hydro-environmental variables and the water level, which means what is happening with the lake in recent years is unknown and there is no certainty regarding their conclusions about the reasons for the lake problem. Therefore, RS-based approaches are more efficient, reliable, and accurate to study climate change and factors affiliated to nature at a large scale with lower cost and less time consumption (Ji & Peters 2003). In this regard, various RS sensors are employed to collect data, among which the Moderate Resolution Imaging Spectroradiometer (MODIS) is the most popular sensor in terms of climate studies to collect vegetation cover and temperature data (Wan *et al.* 2004).

Hydro-environmental processes contain many variables in nature, among which, vegetation cover, temperature, evapotranspiration, and precipitation are the most attention-getting ones to solve water resources problems. Among the vegetation indices, Normalized Difference Vegetation Index (NDVI) is most often used to monitor and model environmental conditions and to study vegetation situations (e.g., see Kalisa *et al.* 2019; Huang *et al.* 2020; Li *et al.* 2020). Land Surface Temperature (LST) is a remotely sensed temperature index and a climate factor that is widely utilized to study hydro-environmental variables (e.g., see Varouchakis 2018; Chen *et al.* 2019; Ren & Liu 2019). Recently, researchers have used different RS sensors to collect data on precipitation amounts. The Tropical Rainfall Measuring Mission (TRMM) Multisatellite Precipitation Analysis (TMPA) provides a calibration-based scheme for combining multiple satellites' precipitation estimates (Zhong *et al.* 2019). After precipitation, evapotranspiration (ET) is the most important factor in the surface hydrologic cycles, and it can be an indicator of the vegetation growth because all water taken up by vegetation is evapotranspired. In recent years, a great number of global ET products have become available from various satellite microwave sensors. Most of the ET datasets are validated using ground-based data (Jackson *et al.* 2010). From the year 2000, the Noah model from the Global Land Data Assimilation System (GLDAS) has provided ET, and other land surface variables (Dorigo *et al.* 2010). Recently, researchers have been using the data produced by GLDAS for hydrologic studies (e.g., see Awange *et al.* 2014; Lv *et al.* 2017; Sehler *et al.* 2019; Zhang *et al.* 2020). Over the past decade, several studies have indicated that water level can be estimated using satellite radar altimetry instead of ground measurements with reasonable accuracy (e.g., see Awange *et al.* 2013; Cai *et al.* 2016; Carabajal & Boy 2020; Zaidi *et al.* 2020). Among radar altimetry datasets, the multi-satellite altimetry dataset of the Radar Altimeter Database System (RADS), which provides different orbit altitudes and geophysical corrections of water level for seas and lakes, is mostly used in studies related to water-level problems (e.g., see Cai *et al.* 2016; Din *et al.* 2019; Rose *et al.* 2019).

Nowadays, new black-box approaches known as artificial intelligence (AI) methods are widely used for assessment of environmental and hydrologic processes. In various aspects of hydrology, AI models such as artificial neural network (ANN) are employed. Recent literature has reported numerous applications of ANNs for monitoring and estimation of hydro-environmental variables (e.g., see Bomers *et al.* 2019; Nourani *et al.* 2019; Dehghanian *et al.* 2020).

In recent years, researchers have tried to detect the effects of potential climate change on big lakes. According to previous studies, long-term trends in hydro-environmental variables can be the reason for spatial-temporal changes in surface water contents. The intensification of the cycles related to hydrology is one of the explicit effects of changes in the behavior of climate factors (Zhang *et al.* 2009). Mann–Kendall (MK) trend test is one of the popular approaches among statistical methods which is used to analyze hydro-environmental time series (e.g., see Nourani *et al.* 2018; Ma *et al.* 2019; Bian *et al.* 2020). Although statistical methods work based on the stationary mode of the given time series, most of the hydro-environmental signals are non-stationary and show non-linear, periodic properties which means that the methods are not suitable to analyze them and the methods should be combined with other approaches (Karpouzos *et al.* 2010).

Wavelet transform (WT) is widely used to decompose the signals with either high or low frequency (e.g., see Roushangar *et al.* 2018; Nalley *et al.* 2020; Nourani *et al.* 2020). The classical signal analysis methods, including

Downloaded from http://iwaponline.com/hr/article-pdf/52/1/176/846791/nh0520176.pdf
by guest

Fourier transform (FT), use a single-window analysis which leads to losing the frequency localizations at low frequency and the time localization at high frequencies. The WT decomposes a one-dimensional signal into two-dimensional time-frequency domains. Also, the irregular shapes of the mother wavelets make the method useful to study the time series with noises and discontinuities (Drago & Boxall 2002). The signals produced by nature, due to its complicated behaviors, are always difficult to study without using machine learning tools. WT can reveal various aspects of datasets, including discontinuities, trends, short- and long-term periodic intervals, and breakdown points, especially in long-term, complex signals.

The current study aimed to determine the main reason for the water-level decline problem of Lake Urmia using RS tools, ANNs, wavelet approaches, and trend test techniques as a high research priority for water resources engineering and management. To this end, RS tools were utilized to collect the hydro-environmental datasets from 1995 to 2019, and ANNs were employed to estimate the missing data. Thereafter, wavelet approaches were used to determine the most dominant periodicity over the basin for the water management plans. The Mann–Kendall trend tests were, also, utilized to study potential trends in the time series. Conclusions based on the fundamental hydrology theories are important in solving the controversial problems of water resources.

Water-level fluctuation is among the common hydrologic problems for big lakes across the world. These changes are mostly associated with climate change and anthropogenic activities. It is very important to determine the main reason for the fluctuations in order to make effective decisions in water resources management. The proposed methodology can be applied to other big lakes across the world in order to investigate potential impacts of climate change and regional human activities on them and, also, to determine the most dominant periodicities of the hydro-environmental variables over the basins.

MATERIALS AND METHODS

Case study

Located in the northwestern part of Iran (Figure 1), between 37°4′ to 38°17′ latitude and 45°13′ to 46° longitude, Lake Urmia is a saline and shallow lake. The lake was among the largest lakes and the second hypersaline lake in the

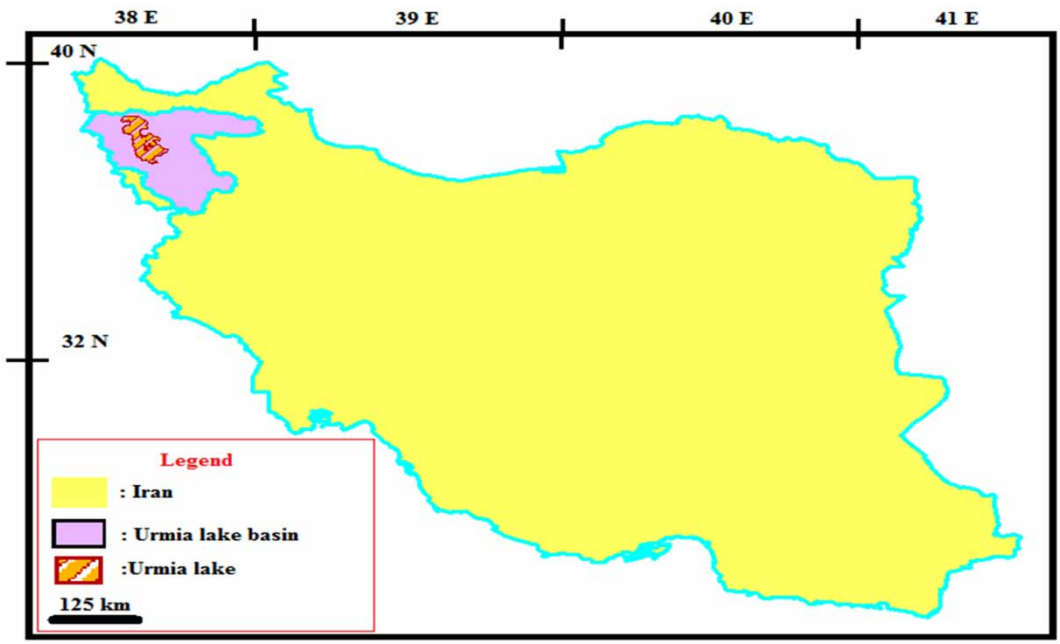

Figure 1 | Lake Urmia location.

Downloaded from http://iwaponline.com/hr/article-pdf/52/1/176/846791/nh0520176.pdf
by guest

world. According to the statistics, the lives of about seven million people depend on their relationship with the lake and that is why Lake Urmia has an important socio-economic role in the country. The Lake Urmia basin is mainly surrounded by mountains and it makes the climate of the region harsh and continental. In recent years, the lake has lost 6 m of its depth out of 16 m (Delju *et al.* 2013). The annual average precipitation in the region is 341 mm and the minimum and maximum temperatures are −23 °C and 39 °C, respectively (Iran Meteorological Observation (IRIMO)). The area of the lake was about 5,650 and 4,610 km^2 in 1998 and 2001, respectively, and the normal catchment area of Lake Urmia is almost 51,676 km^2 (Lake Urmia Basin Integrated Water Resources Management (IWRM)). In the past years, the lake's water level has been decreasing and a quarter of the lake has become saline.

Figure 2 shows the water-level fluctuations for Lake Urmia from 1965 to 2015 (IWRM) and indicates a more than 8 m decline in water level from 1995 to 2015.

Data collection

The present paper employed RS tools, RS-based datasets, and RS-based models to collect data for hydro-environmental indices and factors, and the water-level data to study precipitation, temperature, vegetation cover, and evapotranspiration of Lake Urmia from 1995 to 2019. All of the RS-based datasets were validated using ground-based measurements.

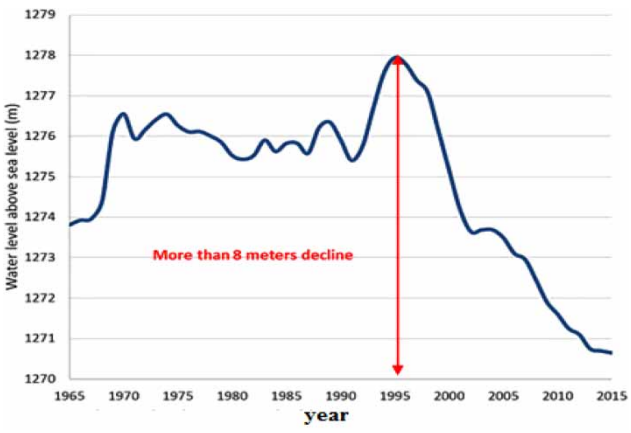

Figure 2 | Water-level fluctuation of Lake Urmia (1965–2015).

NDVI is one of the important indexes that researchers use to evaluate vegetation. The structural basis of this index is the presence of chlorophyll in different plants, which absorbs red light, also, the mesospheric layer of the leaf reflects near-infrared (NIR) light. This index well exhibits the response to photosynthetic effects, with higher values indicating denser and fresher vegetation, that greatly influence environmental parameters. Plants and their roots affect the physical properties of soil, such as moisture content, infiltration rate, and shear strength, which play a significant role in environmental conditions. NDVI is a normalized parameter and its value ranges between −1 and 1. The general equation of the NDVI is (Pettorelli *et al.* 2005):

$$NDVI = (N - D)/(N + R) \quad (1)$$

where N and R denote the near-infrared band and the red band, respectively.

The NDVI dataset from satellite imagery was used and the dataset was collected using vegetation index product of the MODIS (MOD13A1v006).

Temperature data (LST) was extracted using another product (MOD11A1) of MODIS. LST is an important parameter in land surface physics and energy flux between the Earth and atmosphere. LST is utilized in a wide range of hydrology and environment sciences and studies, particularly in projects in which a wide view of the location is needed. Surface temperature is very important in environmental studies because it measures the temperature in the air close to the Earth's surface. Air gets warm owing to radiation exchange from land to the atmosphere. LST as a RS-based index is used to monitor climate and understanding the hydro-environmental conditions (Sobrino *et al.* 1991).

To collect the precipitation dataset, TMPA3B43 product was utilized, which creates a monthly precipitation average, released by the TRMM. The TRMM, launched in 1997, carries several instruments including the Visible Infrared Radiometer (VIRS), TRMM Microwave Imager (TMI), Cloud and Earth Radiant Energy Sensor (CERES), Lightning Imaging Sensor (LIS), and a precipitation radar (PR) and uses different techniques to provide precipitation data using satellite observations. The multi-satellite TMPA

Downloaded from http://iwaponline.com/hr/article-pdf/52/1/176/846791/nh0520176.pdf
by guest

algorithm combines satellite-based observations, infrared sensors, and ground rainfall gauges' analysis in order to produce 3-hourly rainfall estimates. Although the TRMM mission has come to an end and the spacecraft returned to the Earth's atmosphere, the TMPA continues to provide data using inputs from other satellites (Fang *et al.* 2019).

The GLDAS model was used to calculate the ET over the Lake Urmia basin. GLDAS combines satellite and observed data in advanced land surface models to provide land surface data from 1948. The GLDAS data contain hydrological, environmental, and meteorological variables. The data validation indicated that the model can be used in Iran for water resources engineering and management studies (Moghim 2020).

The RADS as an altimetry dataset was employed to collect data for the water level of the lake. The RADS dataset, which was launched by the Delft Institute for Earth-oriented space research at the Delft University of Technology, is based on TOPEX/Poseidon/Jason satellite series (at 10-day resolution), the ERS/ENVISAT/SARAL series (at 35-day resolution), or the Sentinel-3 series (at 27-day resolution) (Cai *et al.* 2016).

Proposed methodology

The current paper aimed to investigate potential trends in the long-term hydro-environmental time series and to analyze the interactions between them and the water-level fluctuations of Lake Urmia. In this way, RS instruments were used to collect data for NDVI, LST, precipitation, and ET over the Lake Urmia basin, and the water-level fluctuations of the lake during 1995–2019. WT, then, was used to decompose the hydro-environmental signals into sub-signals with different frequencies in order to find the most dominant periodicity of the variables over the basin. Thereafter, MK tests were employed as trend test techniques to study potential trends in original time series and their components. MATLAB 2016a was utilized in this study.

Artificial neural networks

A major problem of using RS tools is the lack of data for old years. When it came to the current study, the data collection of MOD13A1 for NDVI started from 2000 and it did not provide NDVI data for 1995–2000. To address this problem, an ANN was designed to predict the NDVI dataset for 1995–2000. In recent decades, the unique features of the human brain have led researchers to simulate the abilities of the human brain with computers. ANNs are dynamical systems that transfer the knowledge or rule behind data to a network structure through processing the empirical data. The input, hidden, and output layers are the main layers of an ANN. Each layer contains a group of neurons that commonly communicate with all neurons in the other layers. Each input in a neural network has its corresponding weight, which enters the transfer function under the influence of this weight and with the purpose of processing and producing inputs of subsequent layers (Nourani *et al.* 2014). It has already been shown that the most widely used neural network in hydrologic studies is a feed-forward neural network (FFNN). The output of an FFNN can be calculated as:

$$\hat{y}_k = f_o\left[\sum_{j=1}^{M_N} W_{kj} \cdot f_h\left(\sum_{i=1}^{N_N} W_{ij} X_i + W_{jo}\right) + W_{ko}\right] \quad (2)$$

In Equation (2), W_{ji} exerted to a hidden layer neuron which connects the ith input neuron to the jth neuron of the hidden layer; W_{jo} is the exerted bias to the jth hidden neuron; f_h shows the activation function of the related hidden neuron; W_{kj} denotes the exerted weight to a neuron of output layer which connects the jth neuron of hidden layer to the kth neuron of output layer; W_{ko} is the exerted bias to the kth neuron of the output layer; f_o indicates output neuron activation function; x_i is the ith neuron of the input layer, and, $\hat{y}_k$ and y is the network estimated and evaluated values, respectively. N_N and M_N indicate the number of neurons in input and hidden layers, respectively. Output and hidden layers have different weights and should be calculated within the training phase (to read more about artificial neural networks please see Nourani *et al.* (2014)).

To assess the performance of the model, determination coefficient (DC) and root mean square error (RMSE)

Downloaded from http://iwaponline.com/hr/article-pdf/52/1/176/846791/nh0520176.pdf
by guest

efficiency criteria were used as Equations (3) and (4) (Nourani 2017).

$$DC = 1 - \frac{\sum_{i=1}^{n} (NDVI_{eval_i} - NDVI_{est_i})^2}{\sum_{i=1}^{n} (NDVI_{eval_i} - \overline{NDVI}_{eval})^2} \quad (3)$$

$$RMSE = \sqrt{\frac{\sum_{i=1}^{n} (NDVI_{eval_i} - NDVI_{est_i})^2}{n}} \quad (4)$$

where n, $NDVI_{eval_i}$, $\overline{NDVI}_{eval}$, and $NDVI_{est_i}$ are, respectively, the number of years, averaged value of the evaluated NDVI (via the instrument), and estimated NDVI.

Autocorrelation analysis

Autocorrelation analysis should be applied to time series in order to study the seasonality patterns and correlations. The results of the trend analysis of time series can be a misunderstanding if a significant autocorrelation has been presented in the time series since it can change the variance which will cause a change in the dispersion of data distribution. Altering the dispersion of data distribution increases the risk of founding a significant trend in the dataset while there is no such trend (Nalley *et al.* 2012). The monthly and seasonal visions of data are expected to have more autocorrelation issues than the annual timescale. Lag-1 autocorrelation coefficient was used to assess autocorrelation for hydrological time series which is calculated as (Yue *et al.* 2002):

$$R = \frac{\left(\frac{1}{n} - 1\right) \sum_{t=1}^{n-1} [x_t - \overline{x_t}][x_{t+1} - \overline{x_t}]}{\left(\frac{1}{n}\right) \sum_{t=1}^{n} [x_t - \overline{x_t}]^2} \quad (5)$$

$$\frac{\{-1 - 1.645\sqrt{n} - 2\}}{n-1} \leq R \leq \frac{\{-1 + 1.645\sqrt{n} - 1\}}{n-1} \quad (6)$$

where R is the autocorrelation coefficient of the sample, x_t, x_t is the mean value of the sample, and n is the number of samples. If R satisfies Equation (6), there is not a significant autocorrelation in the dataset. In the case of the appearance of a significant autocorrelation, Nourani *et al.* (2015) suggested using the pre-whitening MK test instead of the original MK.

Wavelet transform

The WT decomposes a non-stationary signal into multiple levels by shifting and scaling the mother wavelet and using high- and low-pass filters. WTs can analyze data on a local scale and reveal various aspects of the dataset at different frequencies. WTs are widely used in hydro-environmental studies due to their robust properties (Nalley *et al.* 2012). Generally, the WT is sorted into two main classes: discrete wavelet transform (DWT) and continuous wavelet transform (CWT). DWT is often used to decompose hydrologic time series because of the discrete instincts of hydrologic variables. DWT decomposes the signals into the approximation and detail components using high-pass and low-pass filters. The high-pass filter is the wavelet function that produces the detailed sub-signals which are low-scale or high-frequency components of the original signal. The low-pass filter is the scaling function, which produces the approximate coefficient which is the low-frequency or the large-scale of the original signal (Nalley *et al.* 2012). DWT is defined as:

$$\Psi_{m,n}(t) = \frac{1}{\sqrt{a_0^m}} \Psi\left(\frac{t - nb_0 a_0^m}{a_0^m}\right) \quad (7)$$

where $\Psi(t)$ is called the mother wavelet, and a and b are the numbers that control the wavelet dilation and translation, respectively. a_0 and b_0 are a dilation step greater than 1, and the location parameter greater than 0.

The mother wavelet function for DWT at timescale is generally defined as (Nourani *et al.* 2018):

$$\Psi_{a,b}(t) = \frac{1}{\sqrt{a}} \Psi\left(\frac{t-a}{b}\right) \quad (8)$$

where t represents time, and the parameters $a = 2^m$ and $b = a \times n$ are the scaling parameter and the location parameter, respectively.

DWT is performed at dyadic scales in hydro-environmental studies and the wavelet function for this method is (Nourani *et al.* 2018):

$$\Psi_{m,n}(t) = 2^{-\frac{m}{2}} \Psi(2^{-m_t} - n) \quad (9)$$

Downloaded from http://iwaponline.com/hr/article-pdf/52/1/176/846791/nh0520176.pdf
by guest

Therefore, the DWT for discrete signals ($f_i(t)$) can be defined as (Nourani *et al.* 2018):

$$T_i(m,n) = \sum_{i=0}^{N-1} \Psi_i.(t) f_i(t) = 2^{-m/2} \sum_{i=0}^{N-1} \Psi(2^{-m_i} - n) f_i(t) \quad (10)$$

where $T_i(m,n)$ is the WT coefficient at level m for the sample n, and N is an integer in the power of two.

Original Mann–Kendall trend test (MK1)

The MK test is widely used in hydrologic, climatologic, and environmental studies because the test does not require the dataset to have any kind of statistical distributions (Nourani *et al.* 2015). The MK trend test is based on the assumption that the samples in the dataset are independent. A positive or negative trend in a dataset is indicated by computing the MK S-statistics which can yield a positive or negative value as (Hirsch & Slack 1984):

$$S = \sum_{i=1}^{n-1} \sum_{j=i+1}^{n} sgn(x_j - x_i) \quad (11)$$

$$sgn(x_j - x_i) = \begin{cases} 1 & if \quad x_j - x_i > 0 \\ 0 & if \quad x_j - x_i = 0 \\ -1 & if \quad x_j - x_i < 0 \end{cases} \quad (12)$$

where n is the number of samples and x_j stands for the data point at the time j.

The null-hypothesis of the MK test is no-trend, therefore, S is normally distributed with mean = 0 and the variance (σ) is calculated as (Rashid *et al.* 2015):

$$\sigma = \frac{[n(n-1)(2n+5) - \sum d(d-1)(2d+5)}{18} \quad (13)$$

where summation is over the ties and d is the extent of any tie. When the observations are not repeated, d equals to 0.

Thereafter, when the continuity correction is applied, the S-statistic becomes $\overset{'}{S} = S - sgn(S)$, with a normal distribution. For testing the no-trend hypothesis, the Z-value associated with S-statistics of the test is defined as:

$$Z = \frac{\overset{'}{S}}{\sqrt{\sigma}} \quad (14)$$

High positive values of Z denote a positive trend and low negative values indicate a negative trend. The magnitude of the Z-value, also, represents the strength of the trend in the dataset. The probability value (p-value) obtained from the Z-value is used to determine the significance of a trend. In the conditions that p-value is less than pre-determined significant level (here, $\alpha = 5\%$) or greater than the confidence level (here, = 95%), the null hypothesis of no trend is not acceptable (Rashid *et al.* 2015).

The pre-whitening Mann–Kendall test (MK2)

The pre-whitening Mann–Kendall test (MK2) proposes to first remove the autocorrelation such as lag-one or higher processes from the dataset and, then, apply the test. This method is called pre-whitening and is beneficial in terms of high autocorrelation (Burn & Hag Elnur 2002). According to Yue *et al.* (2002), the method contains four major steps:

1. Calculating the slope of the sample data (β) as:

$$\beta = Median\left(\frac{x_i - x_j}{i - j}\right) \quad (15)$$

where x_i and x_j are the ith and jth observation of the dataset.

Then, remove the trend from data as:

$$\overset{'}{X}_i = X_i - (\beta \times i) \quad (16)$$

2. Compute the autocorrelation of the de-trended data as in section 'Autocorrelation analysis'.
3. Remove the autoregressive component from the new dataset to get a residual time series as:

$$\overset{'}{y}_i = \overset{'}{X}_i - (R \times \overset{'}{X}_{i-1}) \quad (17)$$

4. Add the trend back to the residual series as:

$$y_i = \overset{'}{y}_i + (\beta \times i) \quad (18)$$

Wavelet transform–Mann–Kendall method

The WTMK technique contains two main steps. As the first step, DWT is applied to each signal in order to decompose it

Downloaded from http://iwaponline.com/hr/article-pdf/52/1/176/846791/nh0520176.pdf
by guest

into its components. Choosing the best mother wavelet and the level of decomposition are important parts of this step. The appropriate mother wavelet can be selected according to the similarity between the shape of the time series and that of the mother wavelet. Recent literature recommended Daubechies function as an appropriate mother wavelet to decompose hydrological signals due to the shape of the Daubechies function that can cover the limbs of the hydrologic time series (Nourani *et al.* 2015).

Finding the best decomposition level is controversial among researchers and they suggest decomposing the datasets based on their noises which are revealed after each decomposing level. The number of decomposition levels is based on the number of samples in the dataset, as well as the used mother wavelet. The number should be chosen in a way that it corresponds to the data points at which the filter length becomes larger than the last sub-signal (de Artigas *et al.* 2006). Wang & Ding (2003) suggested finding the minimum required decomposition level as:

$$M = INT(\log n) \tag{19}$$

where n and INT are the length of the time series and integer number, respectively.

Moreover, to avoid unnecessary levels of decomposition, de Artigas *et al.* (2006) proposed a method to find the maximum decomposition level as:

$$L = \frac{\log\left(\frac{n}{2v-1}\right)}{\log(2)} \tag{20}$$

where L stands for the maximum number of decomposition levels, v is the number of vanishing moments of a Daubechies wavelet function which is half of its starting length, and n stands for the number of data points in a time series.

The current study utilized smooth Daubechies wavelet functions (db5–db10) because smoother functions are gradual and can represent slowly changing processes, and that is why they are used to investigate long-term time-varying behaviors such as the behavior of hydrological variables. The length of the time series for a monthly viewpoint, for example, is 300, so according to Equation (19), the minimum required decomposition level is 2. Also, with the smoother db functions, the maximum level of decomposition, according to Equation (20), is between 3.98 and 5.05 (for monthly scale), 2.39 and 3.47 (for seasonal scale), and 0.39 and 1.47 (for annual scale). Therefore, three, four, and five levels, and two, three, and four levels, and one and two levels of decomposition were tried for monthly, seasonal, and annual time series, respectively.

According to the above-mentioned theories, four and five levels, and two and three levels of decomposition were used for monthly and seasonal time series, respectively. All smooth mother wavelets (db5–db10) were applied to the signals to determine the more appropriate one in terms of the lowest mean relative error (MRE). The MRE can be calculated as (de Artigas *et al.* 2006):

$$MRE = \frac{1}{n}\sum_{j=1}^{n}\frac{|a_j - x_j|}{|x_j|} \tag{21}$$

where n is the number of records of a signal with x_j original data value, and a_j is the approximation component of x_j.

For the monthly timescales of the hydro-environmental datasets, the lowest MRE was generally obtained for five levels of decomposition when the different db functions for three, four, and five levels of decomposition for each signal were applied. Therefore, five levels of decomposition were chosen to decompose the signals with a monthly horizon using DWT (db types vary from one variable to another). Thereafter, MRE was used to determine the best db to analyze the datasets of each variable. For the monthly dataset of LST, for example, applying different db mother wavelets, produced the lowest MRE using db6 (MRE = 0.46).

Similar procedures were utilized for the seasonal datasets in order to find the best methods to analyze the signals in terms of the lowest MRE. Two, three, and four levels of decomposition were applied to the datasets with the seasonal horizon and four levels of decomposition admitted the lowest MRE. Therefore, four levels of decomposition were applied to the datasets to analyze them using DWT (db types vary from one variable to another). For annual datasets, also, one and two levels of decomposition were applied and the lowest MRE was obtained for two levels of decomposition. Thereafter, the same steps as for monthly and seasonal horizons were

Downloaded from http://iwaponline.com/hr/article-pdf/52/1/176/846791/nh0520176.pdf
by guest

applied to find the best smooth db which varied from one dataset to another.

As the second step of WTMK, the MK trend tests were employed to determine potential trends in approximation and detail components' subseries, as well as the detail components' combination with relevant approximations.

Correlation coefficient

The correlation coefficient (CO) is widely used in data analysis to show the relationship between two datasets. The current study used CO as well as Z-value to determine the most important components in producing trends in the original time series and to find the most dominant hydro-environmental periodicities over the basin. The higher CO value indicates the most efficient component. The CO is calculated as (Nourani *et al.* 2015):

$$CO = \frac{\sum (n - \bar{n})(m - \bar{m})}{\sqrt{\sum (n - \bar{n})^2 \sum (m - \bar{m})^2}} \tag{22}$$

where $\bar{n}$ and $\bar{m}$ are the average of the variables n and m, respectively.

RESULTS AND DISCUSSION

Reviewing the datasets

The current paper used RS tools' instruments to acquire hydro-environmental data over the Lake Urmia basin and the water-level fluctuations of the lake for 1995–2019. In this regard, NDVI, LST, ET, and precipitation datasets were used as hydro-environmental time series to analyze their trends with monthly, seasonal, and annual scales and to study the interactions between these variables and the water-level fluctuations over the past 25 years.

While this study aimed to investigate the hydro-environmental variables for the last 25 years, the MODIS instrument provided data for NDVI only for 2000–2019. In this way, the structure of the FFNN model with the best results in terms of the RMSE and DC was employed as a desirable and optimal structure for modeling to predict the monthly NDVI time series for 1995–2000. In the training phase, the FFNN was trained to learn the relationship between input and output datasets. The input datasets contained LST, ET, and precipitation and the output was NDVI time series from 2001 to 2019 in order to design the FFNN. The FFNN was designed using a scaled conjugate gradient scheme of the back propagation (BP) algorithm considering tangent sigmoid as activation functions, also a trial-and-error procedure was used to determine the best number of neurons in the hidden layer. In the training process, the learning algorithm tries to minimize the error between the targets and the outputs by redistributing the error back through the model. This job is achieved through several iterations and the cycles are known as epoch (Singh *et al.* 2009). The best epoch number for the FFNN was determined as 12 in the validation phase. All of the datasets were normalized before entering the model (Nourani *et al.* 2014). The datasets were randomly separated into three parts, 60% for training the model, 20% for validating, and 20% for testing the performance. The performance for the testing phase with eight hidden layers showed the best results as RMSE = 0.08 and DC = 0.91, and the model was chosen to predict the monthly NDVI time series for 1995–2000.

The NDVI, LST, precipitation, and ET time series over the Lake Urmia basin and the fluctuations of the water level of the lake are illustrated in Figure 3 with a monthly scale from 1995 to 2019. According to the data of the water level above the mean sea level (MSL) (Figure 3(e)), the lake has experienced about a 7 m decline in the water level. The datasets of the hydro-environmental variables (Figure 3(a)–3(d)) had various kinds of patterns with different frequencies which are typical in these datasets. The patterns indicated that the time series were non-stationary; therefore, using the WTMK method would be a beneficial test to investigate the signals of nature. In this way, the WTMK test was used to analyze the hydro-environmental variables and the water level at annual, seasonal, and monthly horizons. First, the autocorrelation of each original, approximation, detail components, and various combinations of sub-series of the hydro-environmental dataset for monthly, seasonal, and annual time-scales were computed in order to determine the lag-one autocorrelation. Table 1 presents the lag-one autocorrelation for original time series. The autocorrelation significances of the other

Downloaded from http://iwaponline.com/hr/article-pdf/52/1/176/846791/nh0520176.pdf
by guest

datasets were controlled using correlograms (examples are given in Figure 4). After using DWT to decompose the original signals into their components, different sub-series were created by combining the approximation with each detail component, separately and the next generations of summations. The combinations helped to reveal signal features via the multi-resolution analysis.

Two MK tests were utilized to detect potential trends in the original time series and the components. The MK1 was used to study the datasets without a significant autocorrelation and MK2 was employed to study the datasets with a statistically significant lag-one autocorrelation.

Results of WTMK technique

The approximation (A), and detail components (D) of the hydro-environmental variables with five, four, and two levels of decomposition for monthly, seasonal, and annual datasets, respectively (the mother wavelets were different from each dataset to another), were collected (an example is given in Figure 5). It is noteworthy that due to the space limitation, the results of all variables and time-scales are not presented graphically. The approximation sub-signal at each time horizon reflected the smoothing trend of the given time series, and the detailed sub-signals represented the various periodicities at different frequencies. Thereafter, the combinations of the approximations with each detail component were used to generate different sub-series.

Then, the MK tests were applied on the original, decomposed, and combinations of sub-series in order to determine potential trends in the time series. Also, CO was computed for each sub-series with the original time series to find the strength of the relation between them. The Z-values and COs of time series for monthly, seasonal, and annual scales are presented in Tables 2–4, respectively. It should be noted that the most dominant periodicities to produce the trends were the compounds with the Z-value close to that of the original time series and the highest CO.

Monthly data analysis

Each monthly time series was decomposed into six components via DWT. The detail sub-series contained five components: 2-month periodicity (D1), 4-month periodicity (D2), 8-month periodicity (D3), 16-month periodicity (D4), and 32-month periodicity (D5) which were high-frequency components and the approximation component (A5) which represented the low frequency or the large scale of the original signal. The lower detail level components represented the higher frequencies to show the rapidly changing behavior of the time series, and the higher-level details had lower frequencies which showed the slowly changing behavior of the original signal. The approximation component (A) represented the slowest changing behavior and the trend of the time series.

According to the results (Table 2), the water level had a significant negative trend in the original dataset (Z-value = −4.3096) which, also, could be seen in its approximation component. The precipitation time series did not have any statistically significant trend (according to the Z-value) in the original signal nor its components. It indicated that the precipitation was almost moderate from 1995 to 2019. Therefore, precipitation could not be the main reason for the water-level decline, although it could be an intensifier factor for the problem. The original NDVI time series (Z-value = 2.5644) and its approximation component (Z-value = 2.0775) had statistically significant positive trends which indicated that the vegetation cover over the basin has increased. The positive trend in NDVI in the condition that precipitation did not have any significant trend showed that agriculture in the basin has occupied a greater area and vegetation health is increased. This conclusion is in agreement with several studies that show water withdrawal is increased in the basin (e.g., see Ashraf *et al.* 2017; Chaudhari *et al.* 2018). According to Table 2, the ET time series had a significant positive trend in the original dataset (Z-value = 2.0565) and its approximation component (Z-value = 2.5814). The positive trends in NDVI and ET in the conditions that the precipitation did not have a significant trend, given the high correlation between vegetation cover and ET according to the previous studies (Khazaei *et al.* 2019), is interesting. As a consequence of fundamental water balance in the basin, the positive trend in the ET time series under positive vegetation trend and stable precipitation situation, the inflow discharge to the lake must have decreased. In this situation, the significant positive trend in the ET time series is due to inefficient or intensive irrigation (Destouni *et al.* 2013). Therefore, inefficient

Downloaded from http://iwaponline.com/hr/article-pdf/52/1/176/846791/nh0520176.pdf
by guest

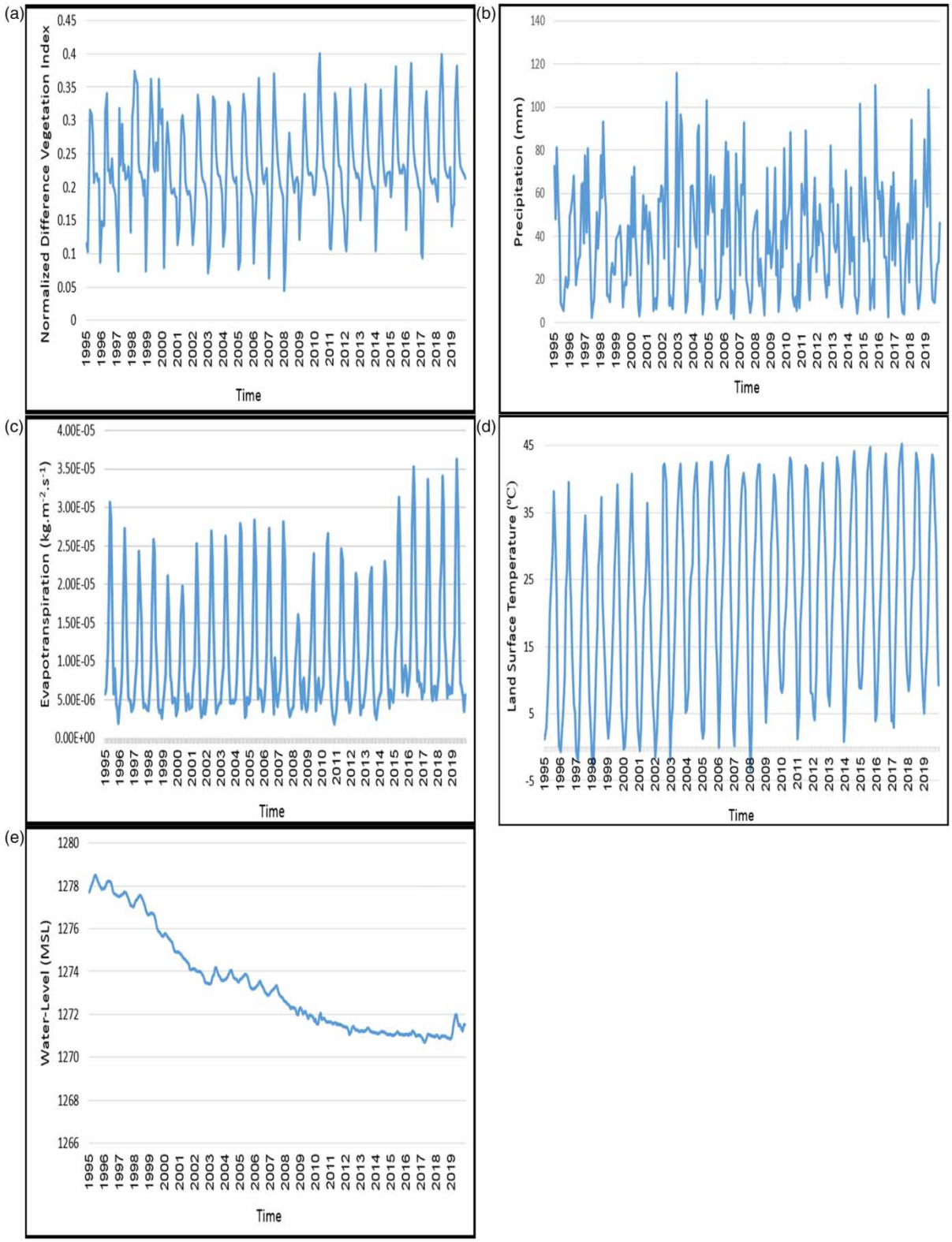

Figure 3 | Monthly time series of (a) NDVI, (b) precipitation, (c) ET, (d) LST, and (e) water level over the Lake Urmia basin during 1995–2019.

Downloaded from http://iwaponline.com/hr/article-pdf/52/1/176/846791/nh0520176.pdf
by guest

Table 1 | Lag-one autocorrelation of the hydro-environmental variables

Variable	Monthly	Seasonal	Annual
LST	**0.8426**[a]	0.0836	**0.8791**[a]
NDVI	**0.6457**[a]	−0.1861	0.2078
Precipitation	**0.4476**[a]	−0.0447	−0.1057
ET	**0.7549**[a]	−0.1191	**0.6496**[a]

[a]The bold values indicate a significant autocorrelation.

irrigation in agriculture is the major reason for the decline in the water level. The LST time series had a statistically significant positive trend (Z-value = 4.9509) in its original dataset which, also, was obvious in the approximation component (Z-value = 3.0495). The positive trend in LST can be another major reason for the decline in water level because it can amplify the evaporation from the surface of the lake and its basin. It is worth mentioning that the significant positive ET and temperature trends which were seen in the basin are in agreement with findings from several other studies (e.g., see Khazaei *et al.* 2019; Schulz *et al.* 2020). It can be seen in Table 2 that the detail components (except for D3 of water level and D2 of LST) did not have a significant trend even for the datasets that their original time series had a statistically significant trend. The approximation component, which is the indicator of trend with low frequency, of the time series with a significant trend, indicated a considerable trend. In some cases, the trend direction of detail components was not in agreement with the original time series, but when the approximation component was added to them, the direction of trend was changed because the approximation component had the most major effect on the original time series and it represented the main trend. This subject supports the theory of adding the approximation to the detail components to have a better interpretation. According to the linear structure of WTs, the next generation of summations have the same behaviors as the first ones. Adding more than one detail component to the approximation showed that the detail component with stronger trend and CO played a leader role for the other ones. The highest CO was seen between the approximation component and the original time series which was another witness to the close relationship between the low-frequency component with the original dataset. Detail components (except for D3 of LST, precipitation, and ET) did not have high values of CO between each of them with their original time series. The high value of CO for D3 in the hydro-environmental variables indicated the high influence of 8-month periodicity over the basin. The dominant detail component was different from one variable to another, which could be due to the different nature of the hydro-environmental variables. The most influential periodicities, generally, were between D1 and D3 (according to the Z-values and COs) which means the main drivers of the trends were the events between 4-month and 16-month in the basin.

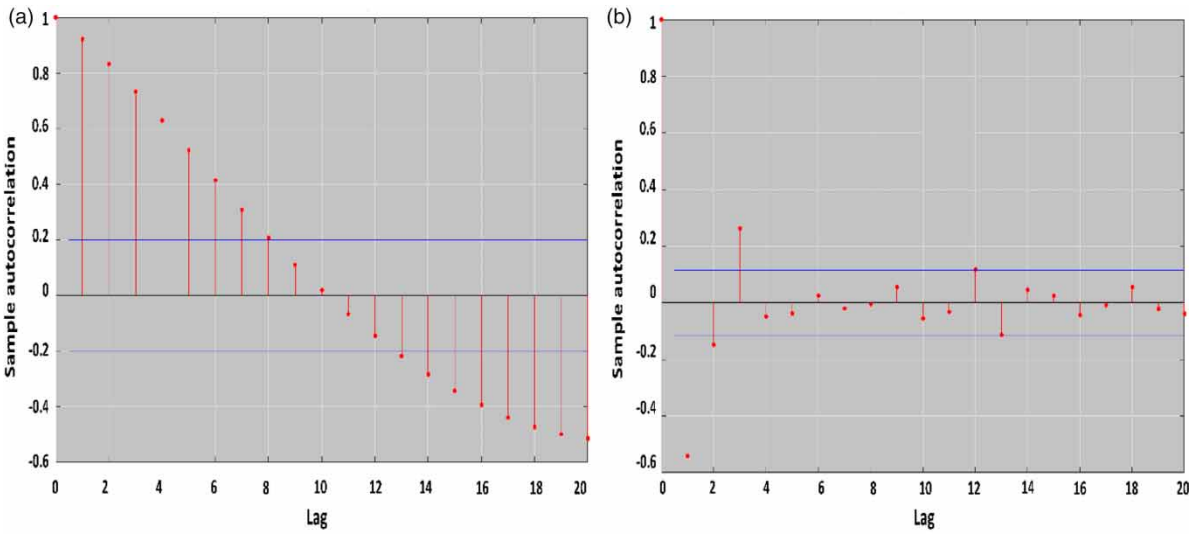

Figure 4 | The correlograms of (a) approximation of (a) seasonal precipitation and (b) D1 of monthly LST.

Downloaded from http://iwaponline.com/hr/article-pdf/52/1/176/846791/nh0520176.pdf
by guest

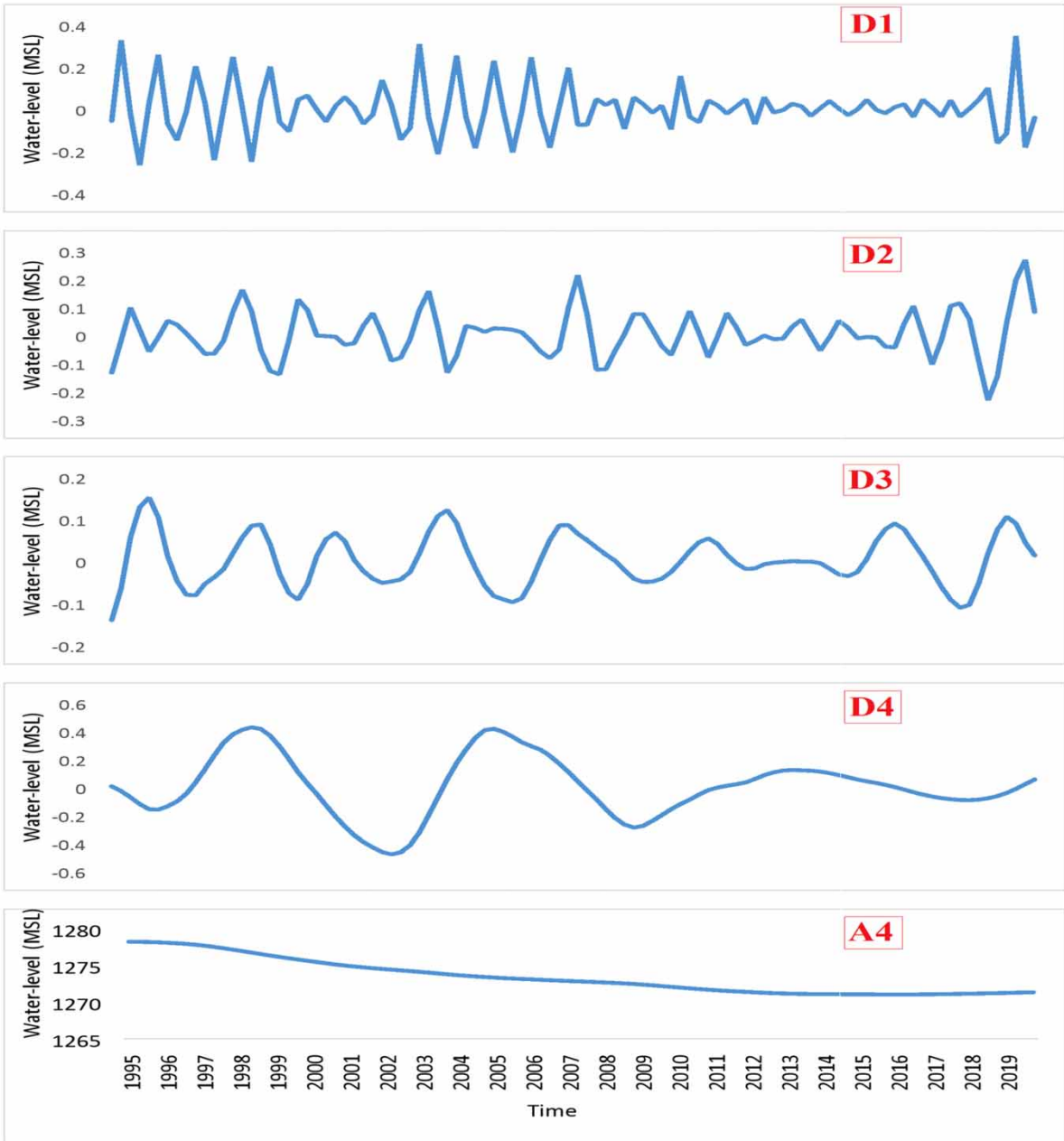

Figure 5 | The approximation (A4) and detail (D1–D4) components of seasonal water level decomposed using db6.

Seasonal data analysis

The presence of annual and seasonal cycles in hydro-environmental signals in monthly-based data analysis showed the need to study the seasonal-based data. Each dataset with seasonal timescale was decomposed into five components including an approximation (A4) and four detail sub-series, 6-month periodicity (D1), 12-month periodicity (D2), 24-month periodicity (D3), and 48-month periodicity (D4). The D2 sub-series with 12-month periodicity could help to explain the trends which were found in the monthly-based analysis, in annual timescale.

According to the results (Table 3), the water level had a significant negative trend in the original dataset

Downloaded from http://iwaponline.com/hr/article-pdf/52/1/176/846791/nh0520176.pdf
by guest

Table 2 | Mann–Kendall Z-values and correlation coefficient (CO) of the monthly time series

	Water level		LST		Precipitation		ET		NDVI	
Time series	**Z-value**	**CO**	**Z-value**	**CO**	**Z-value**	**CO**	**Z-value**	**CO**	**Z-value**	**CO**
Original	**−4.3096**	+	**4.9509**	+	−0.0078	+	**2.0565**	+	**2.5644**	+
A5	**−4.3656**	0.9969	**3.0495**	0.7805	0.6844	0.7349	**2.5814**	0.8491	**2.0775**	0.8712
D1	0.0945	0.0128	0.7967	0.1207	0.0655	0.4594	0.1802	0.2047	0.0800	0.2219
D2	1.0542	0.0192	**−2.5056**	0.3259	0.1529	0.4777	1.6905	0.4480	2.5601	0.1957
D3	**−3.3573**	0.0644	0.2624	0.8675	−0.8202	0.6801	−0.6661	0.8347	−0.2040	0.1439
D4	1.0705	−0.0108	0.0256	0.1704	1.0202	0.2744	0.3436	0.1281	**1.9842**	0.0267
D5	−1.2137	0.0737	−0.5935	0.0799	1.1938	0.1456	−0.8399	0.0758	0.1687	0.0374
A + D1	**−4.3670**	0.9970	**3.2697**	0.6454	0.0949	0.4787	**2.1933**	0.2785	1.5516	0.7347
A + D2	**−4.3602**	0.9973	**4.8642**	0.5997	0.4103	0.4967	**2.4286**	0.7868	1.4585	0.6978
A + D3	**−4.2752**	0.9984	**4.0492**	0.9125	−0.1815	0.6928	1.5514	0.8540	1.3917	0.6841
A + D4	**−4.3814**	0.9974	**3.7374**	0.3227	0.5692	0.3052	1.6218	0.2351	**2.3680**	0.5123
A + D5	**−4.4156**	0.9977	**3.2134**	0.2958	0.2580	0.2003	1.3390	0.1941	1.6540	0.5214
A + D1 + D2	**−4.3507**	0.9971	**4.8460**	0.6210	−0.2292	0.4875	**2.4782**	0.5784	1.5703	0.7103
A + D1 + D3	**−4.2562**	0.9980	**4.2502**	0.8852	−0.6962	0.6192	1.8363	0.6193	1.6931	0.7098
A + D1 + D4	**−4.3777**	0.9972	**3.7801**	0.5584	0.5501	0.4258	**2.1781**	0.2502	**2.2425**	0.6741
A + D1 + D5	**−4.3692**	0.9973	**3.2556**	0.5127	0.2713	0.3289	**1.9890**	0.2215	1.5540	0.6249
A + D2 + D3	**−4.2545**	0.9975	**5.0087**	0.8249	−0.0020	0.5565	**2.0104**	0.8149	1.4127	0.6881
A + D2 + D4	**−4.3428**	0.9973	**4.3268**	0.4561	0.5475	0.4369	**2.5635**	0.5497	**2.0146**	0.5942
A + D2 + D5	**−4.3507**	0.9975	**5.0140**	0.4104	0.9273	0.3127	**2.2812**	0.5123	1.5591	0.5714
A + D3 + D4	**−4.2428**	0.9978	**3.7355**	0.7846	0.0612	0.5268	1.8673	0.6471	**1.9933**	0.5637
A + D3 + D5	**−4.3133**	0.9974	**4.0702**	0.7203	−0.2764	0.4987	1.3232	0.5749	1.2954	0.5789
A + D4 + D5	**−4.3583**	0.9978	**3.6602**	0.3010	0.4836	0.2534	1.9491	0.2213	**2.2170**	0.5197
A + D1 + D2 + D3	**−4.2621**	0.9984	**5.1861**	0.7248	−0.2315	0.6129	**1.9824**	0.7782	1.4987	0.7046
A + D1 + D2 + D4	**−4.3224**	0.9988	**4.2114**	0.5927	0.0904	0.4199	**2.4408**	0.4106	**2.0326**	0.6169
A + D1 + D2 + D5	**−4.3270**	0.9979	**5.0613**	0.5413	−0.0463	0.3273	**2.0133**	0.3987	1.6174	0.6340
A + D2 + D3 + D4	**−4.2483**	0.9987	**4.7640**	0.7314	−0.0680	0.4879	**2.1050**	0.6234	**2.002**	0.6513
A + D2 + D3 + D5	**−4.2914**	0.9980	**5.1122**	0.6120	−0.1438	0.4196	1.8854	0.6031	1.5861	0.6642
A + D2 + D4 + D5	**−4.3236**	0.9989	**4.5118**	0.3947	0.6306	0.3841	**2.5056**	0.4971	**2.0344**	0.5709
A + D3 + D4 + D5	**−4.3049**	0.9990	**3.7585**	0.6403	0.0897	0.4539	1.8894	0.5107	**1.9185**	0.5436
A + D1 + D2 + D3 + D4	**−4.2497**	0.9994	**4.8704**	0.5412	−0.0455	0.5023	**2.2075**	0.5478	**2.1009**	0.6703
A + D1 + D2 + D3 + D5	**−4.2832**	0.9991	**5.0875**	0.6178	−0.2540	0.5742	**2.1602**	0.5274	1.6974	0.6952
A + D2 + D3 + D4 + D5	**−4.3071**	0.9992	**4.9379**	0.6749	0	0.6421	**2.0671**	0.5197	**2.2051**	0.6127

The bold values have statistically significant trends.
The values with underline have a significant autocorrelation and MK2 was used to study their trends.

(Z-value = −3.9656) and the approximation component (Z-value = −3.9278). The LST, ET, and NDVI, again, had significant positive trends in their original time series (Z-values = 2.9066, 2.6350, and 2.1615, respectively). The positive trends in LST and ET were the reasons for the decline in the water level. The precipitation dataset, again, did not have a statistically significant trend. The approximation components showed a high relationship with the original time series (according to the COs) and when the original dataset had a significant trend, the approximations

Downloaded from http://iwaponline.com/hr/article-pdf/52/1/176/846791/nh0520176.pdf
by guest

Table 3 | Mann–Kendall Z-values and correlation coefficient (CO) of the seasonal time series

	Water level		LST		Precipitation		ET		NDVI	
Time series	**Z-value**	**CO**	**Z-value**	**CO**	**Z-value**	**CO**	**Z-value**	**CO**	**Z-value**	**CO**
Original	**−3.9656**	–	**2.9066**	–	−0.2025	–	**2.6350**	–	**2.1615**	–
A4	**−3.9278**	0.9936	**4.0825**	0.7137	0.1705	0.7887	**3.7615**	0.7968	**2.0379**	0.8124
D1	0.0625	0.0721	0.0010	0.3696	−0.1617	0.6435	−0.0522	0.5314	0.5751	0.5666
D2	**−2.4449**	0.7184	**2.1102**	0.8667	−0.1340	0.6882	**2.0745**	0.6389	0.1936	0.9190
D3	0.7146	0.0231	−0.4586	0.1023	0.4317	0.2497	0.1521	0.1561	0.0177	0.1473
D4	−0.5855	0.1428	−0.9541	0.4254	−0.0961	0.1803	0.3525	0.1205	1.1906	0.5416
A + D1	**−3.9507**	0.9947	**3.4171**	0.5914	−0.2642	0.6504	0.7349	0.7571	1.4523	0.5307
A + D2	**−3.9640**	0.9912	**4.0711**	0.8178	−0.2174	0.6912	**2.0638**	0.6683	0.9262	0.7974
A + D3	**−3.9922**	0.9938	**3.3917**	0.5290	0.6275	0.2776	**1.9677**	0.6392	**1.9035**	0.8267
A + D4	**−3.9505**	0.9978	**3.6206**	0.6156	−0.6065	0.2027	**1.9976**	0.6169	**1.9573**	0.8302
A + D1 + D2	**−2.921**	0.9844	**3.8423**	0.7428	−0.2514	0.6642	**1.9845**	0.6048	1.5746	0.6410
A + D1 + D3	**−2.5124**	0.9913	**3.4017**	0.5874	0.2147	0.4967	**1.9874**	0.7159	**2.0367**	0.7068
A + D1 + D4	**−3.0847**	0.9871	**3.5472**	0.6019	−0.7412	0.6045	**2.0173**	0.6987	**1.9767**	0.7243
A + D2 + D3	**−3.9844**	0.9792	**3.7413**	0.6913	0.2014	0.6127	**2.1340**	0.6587	**2.0324**	0.8041
A + D2 + D4	**−3.8131**	0.9901	**3.9127**	0.6874	−0.5873	0.6412	**2.1089**	0.6879	**1.9876**	0.8124
A + D3 + D4	**3.8278**	0.9963	**3.5109**	0.5976	0.0121	0.4546	**1.9974**	0.6245	**2.1059**	0.8234
A + D1 + D2 + D3	**−3.9785**	0.9894	**3.5478**	0.6947	0.1947	0.5978	**2.2478**	0.6201	**2.0179**	0.7125
A + D1 + D2 + D4	**−3.9246**	0.9478	**3.6780**	0.7291	−0.7941	0.5421	**2.1064**	0.6097	**1.9258**	0.6978
A + D1 + D3 + D4	**−3.8843**	0.9903	**3.5078**	0.6098	−0.1247	0.4127	**2.0974**	0.6749	**1.9974**	0.7126
A + D2 + D3 + D4	**−3.9474**	0.9893	**3.6517**	0.6569	0.0231	0.6076	**2.2749**	0.6149	**2.1074**	0.8124

The bold values have statistically significant trends.
The values with underline have a significant autocorrelation and MK2 was used to study their trends.

Table 4 | Mann–Kendall Z-values and correlation coefficient (CO) of the annual time series

	Water level		LST		Precipitation		ET		NDVI	
Time series	**Z-value**	**CO**	**Z-value**	**CO**	**Z-value**	**CO**	**Z-value**	**CO**	**Z-value**	**CO**
Original	**−3.6919**	–	**3.8768**	–	−0.1168	–	**2.6496**	–	**2.2187**	–
A2	**−3.5868**	0.9956	**3.2125**	0.9713	0.6714	0.8385	**2.1540**	0.8538	**2.3452**	0.9214
D1	0.0707	0.0524	1.5128	0.1480	−1.0621	0.7897	0.0593	0.3061	0.6238	0.3419
D2	−0.0276	0.1459	−0.0234	0.1771	−1.0122	0.5298	0.1635	0.4398	0.1773	0.2173
A + D1	**−3.6241**	0.9963	**3.1614**	0.9792	1.0043	0.8582	**1.9944**	0.9319	**2.0977**	0.7464
A + D2	**−3.5957**	0.9991	**3.0983**	0.9918	0.4471	0.6657	**1.9668**	0.9295	**1.9724**	0.6953
A + D1 + D2	**−3.5871**	0.9874	**3.1546**	0.9842	0.9124	0.7421	**2.0127**	0.9475	**1.9987**	0.7124s

The bold values have statistically significant trends.
The values with underline have a significant autocorrelation and MK2 was used to study their trends.

had a significant trend too which was due to the powerful effect of the approximation on the original dataset. An interesting point about the LST was that the trend in the original time series was less than the trend in the approximation component. The negative trends in D3 and D4 showed that 24- and 48-month time modes had made the increasing

Downloaded from http://iwaponline.com/hr/article-pdf/52/1/176/846791/nh0520176.pdf
by guest

temperature a little smoother. Due to the different nature of the hydro-environmental variables, each of them had a special dominant periodicity, but generally speaking, D2 was the dominant component (according to the Z-values and COs) in the basin which means the 12-month periodicity plays an important role in the trends of the original sub-series. This fact revealed the importance of studying the time series in seasonal timescale because the 12-month periodicity was skipped in the monthly-based analysis. D3 and D4, which indicated the components with 24- and 48-month periodicities, showed significant trends when the approximation component was added to them and indicated their effect on the trend of the original time series. The Z-value of the approximation components in some cases not only indicated a significant trend but also was higher than the Z-value of the original time series. These results can be interpreted as a sign for longer-time periodicities over the basin.

Annual data analysis

The possibility of longer-time periodicities' presence which was obvious in monthly- and seasonally-based data analysis as well as the fact that higher-frequency components affect many of the monthly- and seasonally-based datasets, led the study to investigate the lower-frequency components of the time series. Therefore, using DWT, each annually-based dataset was decomposed into two levels with an approximation (A2), and two detail sub-series (D1 and D2). D1 and D2 corresponded to the 2-year and 4-year variations, respectively.

According to the results (Table 4), the water level had a significant negative trend in the original time series (Z-value $= -3.6919$) and the approximation (Z-value $= -3.5868$). The LST, the same as before, had a significant positive trend in the original time series (Z-value $= 3.8768$) and the approximation component (Z-value $= 3.2125$). Precipitation did not have any statistical trend in its dataset. The ET, again, experienced a significant trend in the original dataset and the approximation (Z-values $= 2.6496$ and 2.1540, respectively). The NDVI time series had experienced positive trends in the original and approximation time series (Z-values $= 2.2187$ and 2.3452, respectively). The most dominant periodic components, generally, were D1 and D2, which represented the 2-year and 4-year periodicity.

CONCLUSION

The current paper applied ANNs, wavelet transforms, and Mann–Kendall trend tests to RS-based datasets of the water level, precipitation, LST, NDVI, and ET over the Lake Urmia basin from 1995 to 2019 in order to analyze the time series to determine the most important periodicities of the hydro-environmental variables over the basin and to understand the climate change and human-landscape drivers of the major decline in the water level of Lake Urmia. There were some limitations in this study, which solving them may reveal new aspects of basins to researchers. Studying the water inflow into a lake from rivers which the current study did not have access to could strengthen future studies. As well, investigating groundwater level to study its interactions with the water-level fluctuations of a lake is a suggestion for future studies.

Given the stable condition of the precipitation during the study period, it was concluded that the change in precipitation is not the main reason for the decline in the water level. Instead, a significant positive trend was seen in LST. The increasing temperature will lead to increasing evaporation from the lake's surface and, consequently, it will intensify the decline of the water level. Also, the positive trend in NDVI and ET time series in the conditions that the precipitation was not increasing supported the hypothesis that the human interventions over the basin in terms of agriculture and agricultural activities are the major reasons for the decline in the water level. These conclusions are in agreement with other research experiences over other parts of the world that found human land-use and climate change as the major reasons for the water resources problems.

Although the periodic components that had the major effects on the trends were not the same for all of the hydro-environmental variables, a general conclusion was made. For the monthly-based time series, the components that had frequencies between 4-month and 16-month were found to have the most impact on the trends of the original time series. For the seasonally-based time series, the components with 24- and 48-month frequencies were the most important details for the trend. For the annually-based time series, 2- and 4-year periodicities generated the most important components. The results indicated some useful information about the most important periodicities that affect the

Downloaded from http://iwaponline.com/hr/article-pdf/52/1/176/846791/nh0520176.pdf
by guest

hydro-environmental variables over the Lake Urmia basin which can be considered to model, design, and plan in future studies to help water resources management over the basin.

DATA AVAILABILITY STATEMENT

Data cannot be made publicly available; readers should contact the corresponding author for details.

REFERENCES

Alborzi, A., Mirchi, A., Moftakhari, H., Mallakpour, I., Alian, S., Nazemi, A., Hassanzadeh, E., Mazdiyasni, O., Ashraf, S., Madani, K., Norouzi, H., Azarderakhsh, M., Mehran, A., Sadegh, M., Castelletti, A. & AghaKouchak, A. 2018 Climate-informed environmental inflows to revive a drying lake facing meteorological and anthropogenic droughts. *Environmental Research Letters* **13** (8). https://doi.org/10.1088/1748-9326/aad246

Ashraf, B., Aghakouchak, A., Alizadeh, A., Mousavi Baygi, M., Moftakhari, H. R., Mirchi, A., Anjileli, H. & Madani, K. 2017 Quantifying anthropogenic stress on groundwater resources. *Scientific Reports* **7** (1), 1–9. https://doi.org/10.1038/s41598-017-12877-4.

Awange, J. L., Forootan, E., Kusche, J., Kiema, J. B. K., Omondi, P. A., Heck, B., Fleming, K., Ohanya, S. O. & Gonçalves, R. M. 2013 Understanding the decline of water storage across the Ramser-Lake Naivasha using satellite-based methods. *Advances in Water Resources* **60**, 7–23. https://doi.org/10.1016/j.advwatres.2013.07.002.

Awange, J. L., Gebremichael, M., Forootan, E., Wakbulcho, G., Anyah, R., Ferreira, V. G. & Alemayehu, T. 2014 Characterization of Ethiopian mega hydrogeological regimes using GRACE, TRMM and GLDAS datasets. *Advances in Water Resources* **74**, 64–78. https://doi.org/10.1016/j.advwatres.2014.07.012.

Bian, G., Du, J., Song, M., Zhang, X., Zhang, X., Li, R., Wu, S., Duan, Z. & Xu, C. Y. 2020 Detection and attribution of flood responses to precipitation change and urbanization: a case study in Qinhuai River Basin, Southeast China. *Hydrology Research* **51** (2), 351–365. https://doi.org/10.2166/nh.2020.063.

Bomers, A., van der Meulen, B., Schielen, R. M. J. & Hulscher, S. J. M. H. 2019 Historic flood reconstruction with the use of an artificial neural network. *Water Resources Research* **55** (11), 9673–9688. https://doi.org/10.1029/2019WR025656.

Burn, D. H. & Hag Elnur, M. A. 2002 Detection of hydrologic trends and variability. *Journal of Hydrology* **255** (1–4), 107–122. https://doi.org/10.1016/S0022-1694(01)00514-5.

Cai, Z., Jin, T., Li, C., Ofterdinger, U., Zhang, S., Ding, A. & Li, J. 2016 Is China's fifth-largest inland lake to dry-up? incorporated hydrological and satellite-based methods for forecasting Hulun lake water levels. *Advances in Water Resources* **94**, 185–199. https://doi.org/10.1016/j.advwatres.2016.05.010.

Carabajal, C. C. & Boy, J. P. 2020 Lake and reservoir volume variations in South America from radar altimetry, ICESat laser altimetry, and GRACE time-variable gravity. *Advances in Space Research*. https://doi.org/10.1016/j.asr.2020.04.022

Chaudhari, S., Felfelani, F., Shin, S. & Pokhrel, Y. 2018 Climate and anthropogenic contributions to the desiccation of the second largest saline lake in the twentieth century. *Journal of Hydrology* **560**, 342–353. https://doi.org/10.1016/j.jhydrol.2018.03.034.

Chen, X., Li, F. W., Wang, Y. X., Feng, P. & Yang, R. Z. 2019 Evolution properties between meteorological, agricultural and hydrological droughts and their related driving factors in the Luanhe River basin, China. *Hydrology Research* **50** (4), 1096–1119. https://doi.org/10.2166/nh.2019.141.

de Artigas, M. Z., Elias, A. G. & de Campra, P. F. 2006 Discrete wavelet analysis to assess long-term trends in geomagnetic activity. *Physics and Chemistry of the Earth* **31** (1–3), 77–80. https://doi.org/10.1016/j.pce.2005.03.009.

Dehghanian, N., Saeid Mousavi Nadoushani, S., Saghafian, B. & Damavandi, M. R. 2020 Evaluation of coupled ANN-GA model to prioritize flood source areas in ungauged watersheds. *Hydrology Research* **51** (3), 423–442. https://doi.org/10.2166/nh.2020.141.

Delju, A. H., Ceylan, A., Piguet, E. & Rebetez, M. 2013 Observed climate variability and change in Urmia Lake Basin, Iran. *Theoretical and Applied Climatology* **111** (1–2), 285–296. https://doi.org/10.1007/s00704-012-0651-9.

Destouni, G., Jaramillo, F. & Prieto, C. 2013 Hydroclimatic shifts driven by human water use for food and energy production. *Nature Climate Change* **3** (3), 213–217. https://doi.org/10.1038/nclimate1719.

Din, A. H. M., Zulkifli, N. A., Hamden, M. H. & Aris, W. A. W. 2019 Sea level trend over Malaysian seas from multi-mission satellite altimetry and vertical land motion corrected tidal data. *Advances in Space Research* **63** (11), 3452–3472. https://doi.org/10.1016/j.asr.2019.02.022.

Dorigo, W. A., Scipal, K., Parinussa, R. M., Liu, Y. Y., Wagner, W., De Jeu, R. A. M. & Naeimi, V. 2010 Error characterisation of global active and passive microwave soil moisture datasets. *Hydrology and Earth System Sciences* **14** (12), 2605–2616. https://doi.org/10.5194/hess-14-2605-2010.

Drago, A. F. & Boxall, S. R. 2002 Use of the wavelet transform on hydro-meteorological data. *Physics and Chemistry of the Earth* **27** (32–34), 1387–1399. https://doi.org/10.1016/S1474-7065(02)00076-1.

Erler, A. R., Frey, S. K., Khader, O., d'Orgeville, M., Park, Y. J., Hwang, H. T., Lapen, D. R., Peltier, W. R. & Sudicky, E. A. 2019 Evaluating climate change impacts on soil moisture and

Downloaded from http://iwaponline.com/hr/article-pdf/52/1/176/846791/nh0520176.pdf
by guest

groundwater resources within a lake-affected region. *Water Resources Research* **55** (10), 8142–8163. https://doi.org/10.1029/2018WR023822.

Fang, J., Yang, W., Luan, Y., Du, J., Lin, A. & Zhao, L. 2019 Evaluation of the TRMM 3B42 and GPM IMERG products for extreme precipitation analysis over China. *Atmospheric Research* **223** (March), 24–38. https://doi.org/10.1016/j.atmosres.2019.03.001.

Fathian, F., Dehghan, Z. & Eslamian, S. 2014 Analysis of water level changes in Lake Urmia based on data characteristics and non-parametric test. *International Journal of Hydrology Science and Technology* **4** (1), 18–38. https://doi.org/10.1504/IJHST.2014.064398.

Hassanzadeh, E., Zarghami, M. & Hassanzadeh, Y. 2012 Determining the main factors in declining the Urmia Lake level by using system dynamics modeling. *Water Resources Management* **26** (1), 129–145. https://doi.org/10.1007/s11269-011-9909-8.

Hirsch, R. M. & Slack, J. R. 1984 A nonparametric trend test for seasonal data with serial dependence. *Water Resources Research* **20** (6), 727–732.

Huang, L., Ye, A., Tang, C., Duan, Q. & Zhang, Y. 2020 Impact of rural depopulation and climate change on vegetation, runoff and sediment load in the Gan River basin, China. *Hydrology Research* **2050**, 1–13. https://doi.org/10.2166/nh.2020.120.

Jackson, T. J., Cosh, M. H., Bindlish, R., Starks, P. J., Bosch, D. D., Seyfried, M., Goodrich, D., Moran, M. S. & Du, J. 2010 Validation of advanced microwave scanning radiometer soil moisture products. *IEEE Transactions on Geoscience and Remote Sensing* **48** (12), 4256–4272. https://doi.org/10.1109/TGRS.2010.2051035.

Ji, L. & Peters, A. J. 2003 Assessing vegetation response to drought in the northern Great Plains using vegetation and drought indices. *Remote Sensing of Environment* **87** (1), 85–98. https://doi.org/10.1016/S0034-4257(03)00174-3.

Kalisa, W., Igbawua, T., Henchiri, M., Ali, S., Zhang, S., Bai, Y. & Zhang, J. 2019 Assessment of climate impact on vegetation dynamics over East Africa from 1982 to 2015. *Scientific Reports* **9** (1), 1–20. https://doi.org/10.1038/s41598-019-53150-0.

Karpouzos, D., Kavalieratou, S. & Babajimopoulos, C. 2010 Trend analysis of precipitation data in Pieria Region (Greece). *European Water* **30**, 31–40.

Khazaei, B., Khatami, S., Alemohammad, S. H., Rashidi, L., Wu, C., Madani, K., Kalantari, Z., Destouni, G. & Aghakouchak, A. 2019 Climatic or regionally induced by humans? tracing hydro-climatic and land-use changes to better understand the Lake Urmia tragedy. *Journal of Hydrology* **569**, 203–217. https://doi.org/10.1016/j.jhydrol.2018.12.004.

Li, J., Zhang, S., Huang, L., Zhang, T. & Feng, P. 2020 Drought prediction models driven by meteorological and remote sensing data in Guanzhong Area, China. *Hydrology Research* **51**, 942–958. https://doi.org/10.2166/nh.2020.184.

Liu, X., Zhu, X., Pan, Y., Li, S., Liu, Y. & Ma, Y. 2016 Agricultural drought monitoring: progress, challenges, and prospects. *Journal of Geographical Sciences* **26** (6), 750–767. https://doi.org/10.1007/s11442-016-1297-9.

Lv, M., Ma, Z., Yuan, X., Lv, M., Li, M. & Zheng, Z. 2017 Water budget closure based on GRACE measurements and reconstructed evapotranspiration using GLDAS and water use data for two large densely-populated mid-latitude basins. *Journal of Hydrology* **547**, 585–599. https://doi.org/10.1016/j.jhydrol.2017.02.027.

Ma, C., Fassnacht, S. R. & Kampf, S. K. 2019 How temperature sensor change affects warming trends and modeling: an evaluation across the state of Colorado. *Water Resources Research* **55** (11), 9748–9764. https://doi.org/10.1029/2019WR025921.

Madani, K. 2014 Water management in Iran: what is causing the looming crisis? *Journal of Environmental Studies and Sciences* **4** (4), 315–328. https://doi.org/10.1007/s13412-014-0182-z.

Moghim, S. 2020 Assessment of water storage changes using GRACE and GLDAS. *Water Resources Management* **34** (2), 685–697. https://doi.org/10.1007/s11269-019-02468-5.

Nalley, D., Adamowski, J. & Khalil, B. 2012 Using discrete wavelet transforms to analyze trends in streamflow and precipitation in Quebec and Ontario (1954–2008). *Journal of Hydrology* **475**, 204–228. https://doi.org/10.1016/j.jhydrol.2012.09.049.

Nalley, D., Adamowski, J., Khalil, B. & Biswas, A. 2020 A comparison of conventional and wavelet transform based methods for streamflow record extension. *Journal of Hydrology* **582**, 124503. https://doi.org/10.1016/j.jhydrol.2019.124503.

Nazeri Tahroudi, M., Pourreza-Bilondi, M. & Ramezani, Y. 2019 Toward coupling hydrological and meteorological drought characteristics in Lake Urmia Basin, Iran. *Theoretical and Applied Climatology* **138** (3–4), 1511–1523. https://doi.org/10.1007/s00704-019-02919-4.

Nourani, V. 2017 An emotional ANN (EANN) approach to modeling rainfall-runoff process. *Journal of Hydrology* **544**, 267–277. https://doi.org/10.1016/j.jhydrol.2016.11.033.

Nourani, V., Hosseini Baghanam, A., Adamowski, J. & Kisi, O. 2014 Applications of hybrid wavelet-Artificial intelligence models in hydrology: a review. *Journal of Hydrology* **514**, 358–377. https://doi.org/10.1016/j.jhydrol.2014.03.057.

Nourani, V., Nezamdoost, N., Samadi, M. & Vousoughi, F. D. 2015 Wavelet-based trend analysis of hydrological processes at different timescales. *Journal of Water and Climate Change* **6** (3), 414–435. https://doi.org/10.2166/wcc.2015.043.

Nourani, V., Danandeh Mehr, A. & Azad, N. 2018 Trend analysis of hydroclimatological variables in Urmia lake basin using hybrid wavelet Mann–Kendall and Şen tests. *Environmental Earth Sciences* **77** (5). https://doi.org/10.1007/s12665-018-7390-x

Nourani, V., Jabbarian Paknezhad, N., Sharghi, E. & Khosravi, A. 2019 Estimation of prediction interval in ANN-based multi-GCMs downscaling of hydro-climatologic parameters. *Journal of Hydrology* **579**, 124226. https://doi.org/10.1016/j.jhydrol.2019.124226.

Downloaded from http://iwaponline.com/hr/article-pdf/52/1/176/846791/nh0520176.pdf
by guest

Nourani, V., Farshbaf, A. & Adarsh, S. 2020 Spatial downscaling of radar-derived rainfall field by two-dimensional wavelet transform. *Hydrology Research* **51** (3), 456–469. https://doi.org/10.2166/nh.2020.165.

Pettorelli, N., Vik, J. O., Mysterud, A., Gaillard, J. M., Tucker, C. J. & Stenseth, N. C. 2005 Using the satellite-derived NDVI to assess ecological responses to environmental change. *Trends in Ecology and Evolution* **20** (9), 503–510. https://doi.org/10.1016/j.tree.2005.05.011.

Pokhrel, Y. N., Felfelani, F., Shin, S., Yamada, T. J. & Satoh, Y. 2017 Modeling large-scale human alteration of land surface hydrology and climate. *Geoscience Letters* **4** (1). https://doi.org/10.1186/s40562-017-0076-5

Rashid, M. M., Beecham, S. & Chowdhury, R. K. 2015 Assessment of trends in point rainfall using continuous wavelet transforms. *Advances in Water Resources* **82**, 1–15. https://doi.org/10.1016/j.advwatres.2015.04.006.

Ren, Y. & Liu, S. 2019 A simple regional snow hydrological process-based snow depth model and its application in the Upper Yangtze River Basin. *Hydrology Research* **50** (2), 672–690. https://doi.org/10.2166/nh.2019.079.

Rose, S. K., Andersen, O. B., Passaro, M., Ludwigsen, C. A. & Schwatke, C. 2019 Arctic Ocean sea level record from the complete radar altimetry era: 1991–2018. *Remote Sensing* **11** (14), 1991–2018. https://doi.org/10.3390/rs11141672.

Roushangar, K., Nourani, V. & Alizadeh, F. 2018 A multiscale time-space approach to analyze and categorize the precipitation fluctuation based on the wavelet transform and information theory concept. *Hydrology Research* **49** (3), 724–743. https://doi.org/10.2166/nh.2018.143.

Schulz, S., Darehshouri, S., Hassanzadeh, E., Tajrishy, M. & Schüth, C. 2020 Climate change or irrigated agriculture – what drives the water level decline of Lake Urmia. *Scientific Reports* **10** (1), 1–10. https://doi.org/10.1038/s41598-019-57150-y.

Sehler, R., Li, J., Reager, J. & Ye, H. 2019 Investigating relationship between soil moisture and precipitation globally using remote sensing observations. *Journal of Contemporary Water Research & Education* **168** (1), 106–118. https://doi.org/10.1111/j.1936-704x.2019.03324.x.

Singh, K. P., Basant, A., Malik, A. & Jain, G. 2009 Artificial neural network modeling of the river water quality-a case study. *Ecological Modelling* **220** (6), 888–895. https://doi.org/10.1016/j.ecolmodel.2009.01.004.

Sobrino, J. A., Coll, C. & Caselles, V. 1991 Atmospheric correction for land surface temperature using NOAA-11 AVHRR channels 4 and 5. *Remote Sensing of Environment* **38** (1), 19–34. https://doi.org/10.1016/0034-4257(91)90069-I.

Varouchakis, E. A. 2018 Spatiotemporal geostatistical modelling of groundwater level variations at basin scale: a case study at Crete's Mires Basin. *Hydrology Research* **49** (4), 1131–1142. https://doi.org/10.2166/nh.2017.146.

Wan, Z., Wang, P. & Li, X. 2004 Using MODIS Land Surface Temperature and Normalized Difference Vegetation Index products for monitoring drought in the southern Great Plains, USA. *International Journal of Remote Sensing* **25** (1), 61–72. doi:10.1080/0143116031000115328

Wang, W. & Ding, J. 2003 Wavelet network model and its application to the prediction of hydrology. *Nature and Science* **1** (1), 67–71.

Yue, S., Pilon, P., Phinney, B. & Cavadias, G. 2002 The influence of autocorrelation on the ability to detect trend in hydrological series. *Hydrological Processes* **16** (9), 1807–1829. https://doi.org/10.1002/hyp.1095.

Zaidi, A. Z., Vignudelli, S., Khero, Z., Ghauri, B. M. K., Muzaffer, R., Naeem, B., Panhwar, V., Zafar, S. & ul Haque, S. 2020 Indus river water level monitoring using satellite radar altimetry. *Advances in Space Research*. https://doi.org/10.1016/j.asr.2020.03.044

Zhang, Q., Xu, C. Y., Zhang, Z., Chen, Y. D. & Liu, C. L. 2009 Spatial and temporal variability of precipitation over China, 1951–2005. *Theoretical and Applied Climatology* **95** (1–2), 53–68. https://doi.org/10.1007/s00704-007-0375-4.

Zhang, J., Liu, K. & Wang, M. 2020 Seasonal and interannual variations in China's groundwater based on GRACE data and multisource hydrological models. *Remote Sensing* **12** (5). https://doi.org/10.3390/rs12050845

Zhong, R., Chen, X., Lai, C., Wang, Z., Lian, Y., Yu, H. & Wu, X. 2019 Drought monitoring utility of satellite-based precipitation products across mainland China. *Journal of Hydrology* **568**, 343–359. https://doi.org/10.1016/j.jhydrol.2018.10.072.

First received 2 August 2020; accepted in revised form 30 October 2020. Available online 29 December 2020

Downloaded from http://iwaponline.com/hr/article-pdf/52/1/176/846791/nh0520176.pdf
by guest